
Article:
Garcia, R., Helal, Y., Pilakoutas, K. et al. (1 more author) (2013) Bond strength of short lap splices in RC beams confined with steel stirrups or external CFRP. Materials and Structures. Published Online 9th October 2013. 1 - 17. ISSN 1359-5997

https://doi.org/10.1617/s11527-013-0183-5

Bond strength of short lap splices in RC beams confined with steel stirrups or external CFRP

Reyes Garcia*, Yasser Helal, Kypros Pilakoutas, Maurizio Guadagnini

Dept. of Civil and Structural Engineering, The University of Sheffield, Sir Frederick Mappin Building, Mappin Street, Sheffield, S1 3JD, UK.

Tel.: +44 (0) 114 222 5071

Fax: +44 (0) 114 222 5700

Email (corresponding author*): r.garcia@sheffield.ac.uk

Abstract

This paper investigates the bond behaviour of lapped steel bars using fifteen RC beams tested in flexure. Twelve of the beams were designed to fail by bond splitting at midspan, where the main flexural reinforcement was lapped 10 bar diameters. The parameters studied include the amount and type of confinement at midspan (no confinement, internal steel stirrups or externally bonded carbon FRP), concrete cover and bar size. The results show that the CFRP confinement enhanced the bond strength of the lapped bars by up to 49% with reference to unconfined beams, and improved significantly the overall behaviour of the specimens. The experimental results are compared with existing models to predict the bond strength enhancement provided by CFRP confinement. It is shown that existing models overestimate considerably the CFRP strains and show a large scatter when predicting experimental results. Based on the test results, a new approach to predict the bond strength enhancement due to CFRP confinement is proposed. This can be used during the assessment and strengthening of substandard RC constructions.

Keywords: substandard lap splices, seismic strengthening, RC beams, CFRP confinement, bond-splitting strength, bar slip

1. Introduction

Extensive damage in recent major earthquakes in Mediterranean and developing countries has highlighted the seismic vulnerability of existing substandard RC buildings built with little or no seismic detailing and low quality materials (Kashmir, 2005; China, 2008; Indonesia and Italy, 2009; Haiti, 2010; Turkey,

2011). Many catastrophic failures in these structures can be attributed to failure of inadequately spliced reinforcement at locations of large demand, such as the column-footing interface and above beam-column joints. The local strengthening of these deficient members is a feasible intervention for reducing the seismic vulnerability of substandard buildings. Over the last two decades, externally bonded FRP have been extensively used by engineers for many seismic strengthening applications. Compared to other traditional strengthening techniques, FRP materials offer advantages such as high strength to weight ratio, high resistance to corrosion, excellent durability, ease and speed of in-situ application and flexibility to strengthen selectively only those members seismically deficient (Gdoutos et al. 2000).

Extensive experimental research has confirmed the effectiveness of FRP confinement at improving the behaviour of columns with inadequate short lapped reinforcement (e.g. Saadatmanesh et al. 1996, 1997; Seible et al. 1997; Ma and Xiao 1999; Harajli and Rteil 2004; Harries et al. 2006; Bousias et al. 2006; Breña and Schlick 2007; Youm et al. 2007; Harajli and Dagher 2008; Harajli and Khalil 2008; Elgawady et al. 2010; Elsouri and Harajli 2011; Bournas and Triantafillou 2011). Despite the extensive research effort, only a few design models exist for the strengthening of column splices using FRP materials. Priestley et al. (Priestley and Seible 1995; Seible et al. 1997) proposed the first model for FRP strengthening of short lapped bars in columns, where failure was likely dominated by splitting. Whilst this model is included in current FRP design guidelines such as CNR-DT 200/2004 (CNR 2004) and Eurocode 8 (BSI 2005), its use in actual strengthening applications may lead to very conservative amounts of FRP confinement (Harries et al. 2006; Harajli and Khalil 2008).

More recently, the confinement of lapped bars with FRP materials was investigated by adopting an approach similar to that used for steel confinement (Hamad et al. 2004; Harajli et al. 2004; Tastani and Pantazopoulou 2010; Bournas and Triantafillou 2011). The results of these studies indicate that the full bond strength of the lapped bars could be developed using less FRP confinement than that recommended by current FRP strengthening guidelines. The investigations also show that, in splitting-prone RC members, CFRP confinement is effective at

enhancing bond strength up to the point where pullout of the bars dominates failure. This is also acknowledged in existing bond equations (Orangun et al. 1977; Lettow and Eligehausen 2006; *fib* Model Code 2010), where the maximum bond strength enhancement due to (heavy) steel confinement is limited to maximum 30-40%. Based on the results of a limited number of experiments, some analytical models were proposed to compute the additional contribution of FRP confinement to the bond strength of splices (Hamad et al. 2004; Harajli et al. 2004; Tastani and Pantazopoulou 2010; Bournas and Triantafillou 2011). These models are mainly based on modifications of existing equations originally developed for steel confinement, and assume the total bond strength of a lap as the sum of the individual contributions of concrete cover and FRP confinement. Therefore, the concrete contribution to bond strength is computed using bond strength equations available in the literature, whereas the contribution of the FRP confinement is computed by adopting i) an equivalent area of FRP confinement accounting for the different stiffness of steel stirrups and FRPs (for instance Harajli et al. 2004), or ii) an effective strain that can be developed in the FRP confinement (Hamad et al. 2004; Tastani and Pantazopoulou 2010; Bournas and Triantafillou 2011). Whilst the use of these models may lead to more economical FRP strengthening solutions, it is necessary to evaluate their accuracy using more tests that consider other geometries and test parameters. Moreover, although some of the previous models utilise an effective FRP strain in the calculations, few researchers have studied in detail the development of FRP strains during bond-splitting failures (e.g. Harajli and Dagher 2008) and its interaction with bar slippage during tests.

This paper investigates the effectiveness of externally bonded carbon FRP (CFRP EBR) confinement at enhancing the behaviour of RC beams. To achieve this, fifteen RC beams were tested in flexure. Twelve of these beams were designed to fail by bond-splitting at the midspan, where the main bottom reinforcement was lapped. As a result, the confinement of this zone is expected to improve considerably the “local” bond behaviour of the bars and therefore the overall behaviour of the beams. The results of the experiments are used to examine the accuracy of current predictive models available in the literature. Based on the test results, a new approach to predict more accurately the bond strength enhancement

of short lapped bars in RC members confined with CFRP is proposed. This study is part of a multistage research project focused on the seismic strengthening of substandard RC buildings in developing countries (Garcia et al. 2010; 2012).

2. Experimental programme

2.1 Geometry of beam specimens

A total of fifteen RC beams were tested in flexural four-point bending. The geometry of twelve of these beams simulates a member in flexure with a known spliced length, similar to the specimens tested by Harajli (2006). The beams had a rectangular cross section of 150×200 mm, a total length of 1200 mm and a clear span of 1100 mm as shown in Figure 1a-b. Two 50×100 mm notches at the bottom of the beams defined the lap length and exposed the main flexural bars for measurements. The bottom flexural reinforcement consisted of two steel bars lapped at the midspan zone. Bar sizes of 12 and 16 mm were used as main bottom reinforcement. The top beam reinforcement consisted of two continuous 10 mm bars. To prevent a brittle shear failure, the beam outside of the lapped zone had transversal reinforcement consisting of 6 mm fully closed plain stirrups spaced at 100 mm centres. Due to the relatively short lap length selected for these tests (lap length l_b=10d_b, where d_b is the bar diameter), the reinforcement is expected to remain elastic at failure. The short lap length was designed to lead to bar slippage, but also to allow a significant number of bar ribs (lugs) to participate during bar movement.

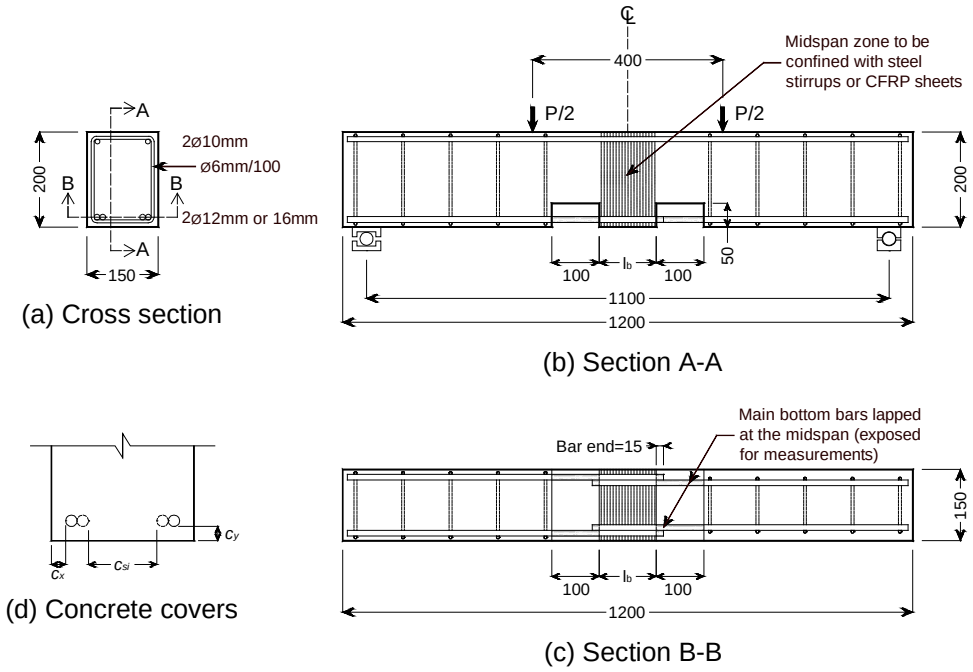

Fig. 1 Geometry and reinforcement details of tested beams

To investigate the concrete to diameter ratio (c/d_b), concrete covers of 10 and 20 mm were selected for the beams reinforced with 12 mm bars, whereas 27 mm was used for the beams reinforced with 16 mm bars. For each beam, the side and bottom covers were chosen to be approximately equal. Two types of confinement were investigated: internal steel stirrups and externally bonded CFRP composites. Hence, three beams were reinforced internally using two 6 mm smooth stirrups at the lapped zone. To replicate old construction practices, the stirrups were closed with 90 degree hooks instead of 135 degree hooks typically required by current seismic codes. The midspan region of three beams was fully wrapped with 1 layer and three beams with 2 layers of externally bonded CFRP sheets. For comparison, three unconfined beams with lapped bars and three benchmark beams with continuous bottom bars were also cast.

The main characteristics of the tested beams are shown in Table 1. The beams are classified in three groups according to the intended concrete cover c (SC10 for c=10 mm, SC20 for c=20 mm, and SC27 for c=27 mm). Individual beams were identified using an ID as follows: B=benchmark beams, Ctrl=unconfined control, S=steel-confined, and F=CFRP-confined beams. The last digit of the CFRP-confined beams indicates the number of layers used to strengthen the midspan region (1 or 2 layers). Table 1 also reports the effective side (c_x), bottom (c_y) and

internal (c_{si}) concrete covers measured after casting (definitions shown in Figure 1d). The measured covers produced c_{min}/d_b ratios ranging from 0.78 to 1.58, where c_{min} is the smaller of c_x, c_y or $c_{si}/2$. These relatively small c_{min}/d_b ratios replicate typical covers of many substandard RC structures in developing countries.

Table 1 Characteristics of tested beams

Group	Beam	f_{cm} (MPa)	Measured cover (mm)			Main bars	Confinement at midspan
			c_x	c_y	c_{si}		
SC10	SC10B	22.5	-	-	-	2Ø12	Ø6/100 mm
	SC10Ctrl	22.5	16	14	69	2Ø12	None
	SC10S	22.5	21	16	60	2Ø12	2Ø6/60 mm
	SC10F1	37.6	17	17	67	2Ø12	1 CFRP layer
	SC10F2	22.5	18	13	67	2Ø12	2 CFRP layers
SC20	SC20B	37.6	-	-	-	2Ø12	Ø6/100 mm
	SC20Ctrl	37.6	19	22	63	2Ø12	None
	SC20S	37.6	20	24	61	2Ø12	2Ø6/60 mm
	SC20F1	37.6	20	22	62	2Ø12	1 CFRP layer
	SC20F2	37.6	20	21	60	2Ø12	2 CFRP layers
SC27	SC27B	37.6	-	-	-	2Ø16	Ø6/100 mm
	SC27Ctrl	37.6	28	27	25	2Ø16	None
	SC27S	37.6	28	26	31	2Ø16	2Ø6/70 mm
	SC27F1	37.6	30	27	27	2Ø16	1 CFRP layer
	SC27F2	37.6	27	31	33	2Ø16	2 CFRP layers

2.2 Material properties

The beams were cast using two batches of ready mixed concrete with a mean target 28-days strength f_{cm}=16/20 MPa. The following mix proportions were reported by the supplier: Portland cement CIIIA=125 kg/m^3, GGBS=125 kg/m^3, coarse aggregate 4-10 mm=1002 kg/m^3, sand 0-4 mm=884 kg/m^3, and water/cement ratio of 0.8. The concrete was cast from the top of the beams so that the lapped reinforcement is classified as bottom cast bars. After casting, the beams were covered with wet hessian and polythene sheets, cured for seven days in the moulds and subsequently stored under standard laboratory conditions.

The concrete properties for each batch are summarised in Table 2. For each batch, the mean concrete compressive strength (f_{cm}) was obtained from tests on at least three 150×300 mm concrete cylinders according to BS EN 12390-3 (BSI 2009a). The indirect tensile splitting strength of concrete (f_{ctm}) was determined from tests on six 100×200 mm cylinders as for BS EN 12390-6 (BSI 2009c). The modulus of rupture (f_{cfm}) was obtained from four-point bending tests on six prisms of 100×100×500 mm according to BS EN 12390-5 (BSI 2009b). Cylinders and prisms were cast at the same time and cured under the same conditions as the beams. The average results and corresponding standard deviations (StdDev) from the tests on cylinders and prisms are reported in Table 2. The elastic moduli (E_{cm}) of concrete calculated according to Eurocode 2 (EC2) (BSI 2004) were 28.1 and 32.7 GPa for batches 1 and 2, respectively.

Table 2 Properties of concrete batches used to cast the beams

Test		Batch 1	Batch 2
Slump (mm)		145	185
Compressive strength (MPa)	Mean	22.5	37.6
	StdDev	1.93	1.64
Indirect tensile strength (MPa)	Mean	2.63	2.81
	StdDev	0.18	0.22
Modulus of rupture (MPa)	Mean	4.53	4.88
	StdDev	0.26	0.22

The main bottom reinforcement of the beams consisted of high ductility ribbed bars Grade 500 complying with BS 4449:2005 (2005) requirements. The mechanical properties of the bars were evaluated by direct tension tests on three bar samples. Yield and ultimate strength were: f_y=559 and f_u=692 MPa for the 12 mm bar, and f_y=551 and f_u=683 MPa for the 16 mm bar. The elastic modulus of both bars was E_s=209 GPa. Yield and ultimate strength of the 6 mm smooth stirrups used as internal confinement were f_y=360 and f_u=420 MPa. Table 3 summarises the bar and rib geometry data provided by the bar manufacturer based on actual measurements on 58 (12 mm) and 245 (16 mm) bar samples.

Table 3 Rib geometry of main lapped bars

Nominal bar size (mm)		12	16
Rib angle α (deg)		35 & 75	35 & 75
Rib face angle β (deg)		50	50
Relative rib area (mm^2)	Mean	0.084	0.087
	StdDev	0.006	0.009
Rib height (mm)	Mean	1.02	1.32
	StdDev	0.07	0.08
Average rib spacing (mm)	Mean	7.40	9.42
	StdDev	0.13	0.17
Cross-section area (mm^2)	Mean	111	196
	StdDev	1.10	2.00

A commercial composite system consisting of unidirectional CFRP sheets and bonding adhesive was used for external strengthening. The mechanical properties of the dry fibres provided by the manufacturer (S&P) were: tensile strength f_f=4000 MPa, modulus of elasticity E_f=240 GPa, ultimate elongation ε_{fu}=1.60%, and fibre thickness t_f=0.117 mm. The properties of the two-component epoxy bonding adhesive were: tensile strength f_{adh}=17 MPa, bond to concrete b_{adh}>4 MPa and modulus of elasticity E_{adh}=5 GPa. Before applying the CFRP confinement, concrete surfaces at the application zones were thoroughly brushed and cleaned with pressurised air to improve the adherence between the existing concrete and the fibre sheets. The sharp corners at the application zone were also rounded off to a radius of approximately 10 mm. An epoxy resin primer was then applied to seal the concrete surface at the application zones. The sheets were oriented perpendicular to the beam axis and were applied across the entire lap length using a wet lay-up technique.

2.2 Instrumentation and test set-up

The beams were tested under displacement-controlled four-point bending in a four-column universal testing machine of 1000 kN capacity. The load was applied symmetrically using a hydraulic actuator and a spreader loading beam as shown in Figure 2a. This loading configuration produced a constant moment over the

lapped bars at the midspan. The beams were simply supported on steel plates and rollers. As the support platen of the universal testing machine was slightly shorter than the beams, a stiff H steel profile was used to support the concrete beams (see Figure 2a).

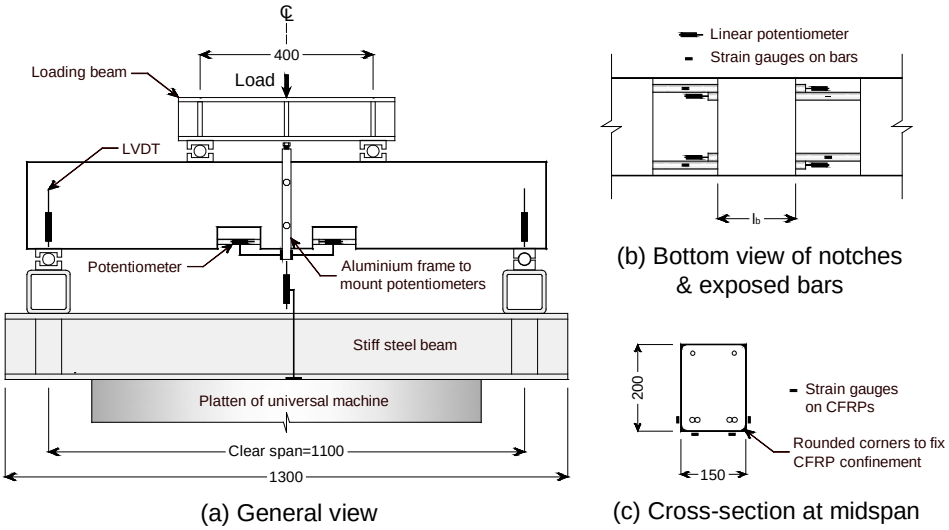

Fig. 2 Typical instrumentation and set-up of tested beams

Two Linear Variable Displacement Transducers (LVDTs) monitored the vertical midspan deflections of the beams. Vertical displacements at the supports were also measured using LVDTs to compute net deflections. Strains along the main lapped bars were measured using four foil-type electrical resistance strain gauges fixed on the reinforcing bars exposed at the notches as shown in Figure 2b. To obtain detailed information of the strains in the CFRP confinement, four strain gauges were fixed on the CFRP at the locations where splitting cracks were expected, as shown in Figure 2c. The slip at the free end of the lapped bars was also monitored using linear potentiometers mounted on an aluminium frame (see Figure 2a-b). The frame was clamped at the centreline of the beam to record the bar slip relative to intact concrete. All beams were tested after 28 days of casting, and 7 days or more after fixing the CFRP confinement.

To check the instrumentation and release any residual stresses in the beams, an initial load of 5.0 kN was applied and then totally released. The initial load was then restored and subsequently increased up to the maximum capacity of the beams. After this point, the confined beams were subjected to three full load-reload cycles (except beams SC10S and SC10F2). Crack development was

monitored at each load increment by visual inspection. The tests were halted when splitting failure occurred (unconfined beams), or when the load-midspan deflection curve was practically horizontal due to a low residual resistance (confined beams).

3. Test results

Table 4 reports the splitting load (P_{spl}) of the tested beams, corresponding midspan deflection (δ_{spl}) at P_{spl}, enhancement in load (ΔP_{spl}) and deflections ($\Delta\delta_{spl}$) of the steel and CFRP-confined beams over the control beams, and the post-split load and deflection at 85% of the splitting load ($P_{spl,85\%}$ and $\delta_{spl,85\%}$, respectively). The table also presents the ratio of maximum load of the tested beams to that of the benchmark beams (P_{spl}/P_{bmk}) and the average bar stress at splitting failure ($f_{s,spl}$). The following sections summarise the most significant observations of the testing programme and discuss the results listed in Table 4.

Table 4 Load, deflection and bar stress results of tested beams

Beam	P_{spl} (kN)	δ_{spl} (mm)	ΔP_{spl} (%)	$\Delta\delta_{spl}$ (%)	$P_{spl,85\%}$ (kN)	$\delta_{spl,85\%}$ (mm)	P_{spl}/P_{bmk} (%)	$f_{s,spl}$ (MPa)
SC10B	98.3	6.89	-	-	-	-	100	464
SC10Ctrl	33.0	0.94	-	-	-	-	33	168
SC10S	36.8	1.52	+11	+62	31.2	2.21	37	190
SC10F1	42.1[(a)]	1.84	+27	+96	35.8[(a)]	2.10	43	223[(a)]
SC10F2	49.1	2.00	+51	+110	41.6	4.05	50	249
SC20B	120	9.22	-	-	-	-	100	561
SC20Ctrl	34.6	1.36	-	-	-	-	29	185
SC20S	39.0	1.82	+13	+34	NA	NA	32	230
SC20F1	47.3	1.91	+37	+40	40.2	2.30	39	239
SC20F2	48.9	1.96	+41	+44	41.5	2.18	40	265
SC27B	156	6.14	-	-	-	-	100	544
SC27Ctrl	52.1	1.37	-	-	-	-	33	171
SC27S	50.0	1.72	-4	+25	42.5	4.13	32	162
SC27F1	68.7	1.89	+31	+38	58.3	7.74	44	214
SC27F2	69.6	1.95	+33	+42	59.1	10.6	45	230

[(a)] Value normalised by $(22.5/37.6)^{1/4}$

3.2 Modes of failure

In all unconfined beams, first flexural cracks were located at the upper corners of the notches outside the splice zone. The beams experienced sudden brittle failure due to splitting of the concrete cover around the lapped bars. This was accompanied by a loud explosive noise and the complete detachment of the cover, which exposed the lapped reinforcement as shown in Figure 3a.

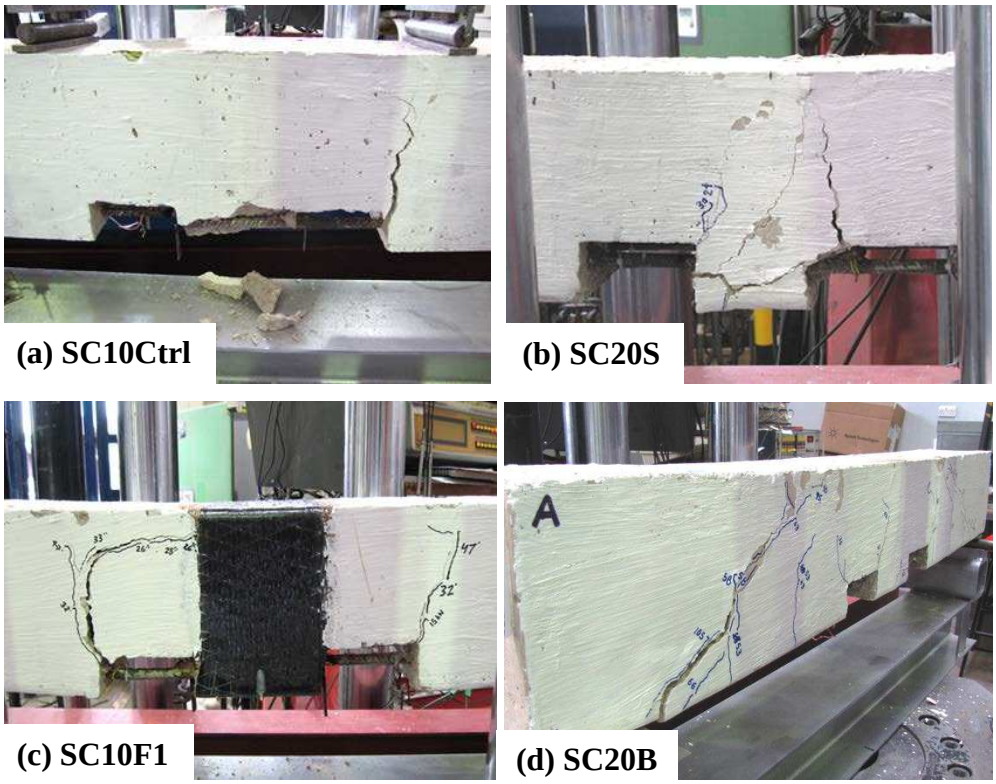

Fig. 3 Typical failures at the midspan of beams: (a) unconfined control, (b) steel-confined, (c) CFRP-confined, and (d) benchmark

The use of internal stirrups in the lapped zone did not delay the onset of flexural cracking of the steel-confined beams. However, unlike the unconfined beams, additional flexural cracks appeared across the constant moment region. At the maximum load, splitting cracks formed along the lapped bars. Figure 3b shows a typical failure of a steel-confined beam. Although the concrete cover did not spall completely, large flexural and splitting cracks formed across the lapped zone.

The initial flexural crack pattern of steel and CFRP-confined beams was similar. However, as the CFRP sheets were bonded directly onto the concrete surface (see Figure 3c), splitting cracks at failure were almost unnoticeable. The CFRP

confinement also reduced significantly the widening of splitting cracks and prevented concrete cover spalling. No evident damage occurred at the CFRP sheets during the tests. However, towards the end of the tests, some local fibre debonding occurred at the location of wide flexural and splitting cracks. It should be mentioned that for beams SC10 and SC20, splitting cracks formed first at the side and bottom concrete covers. Conversely, for beams SC27, concrete splitting occurred first between the lapped bars, and then at the side and bottom covers. This was due to the small internal concrete cover between the lapped bars of the latter beams (approximately 30 mm), which was the smallest cover.

A typical failure mode of the benchmark beams (with continuous flexural reinforcement) is shown in Figure 3d. Although significant flexural cracking occurred within the constant moment zone, the formation of shear cracks close to the supports prevented the beams from reaching higher flexural capacity (except for beam SC20B, which yielded). This type of failure was anticipated as the load arrangement used for the tests produced a small shear span-to-depth ratio between the load points and the beam supports ($a/d \approx 2.0$). Nonetheless, the beams were close to reaching their full flexural capacity and beam SC20B developed some yielding (see bar stresses in Table 4).

3.2 Load-deflection response

The load-deflection responses obtained from the tests are shown in Figures 4a-c. In Figure 4a, the load of beam SC10F1 (which had a higher concrete strength) is normalised by $(22.5/37.6)^{1/4}$, as proposed by Zuo and Darwin (2000) and Hamad et al. (2004).

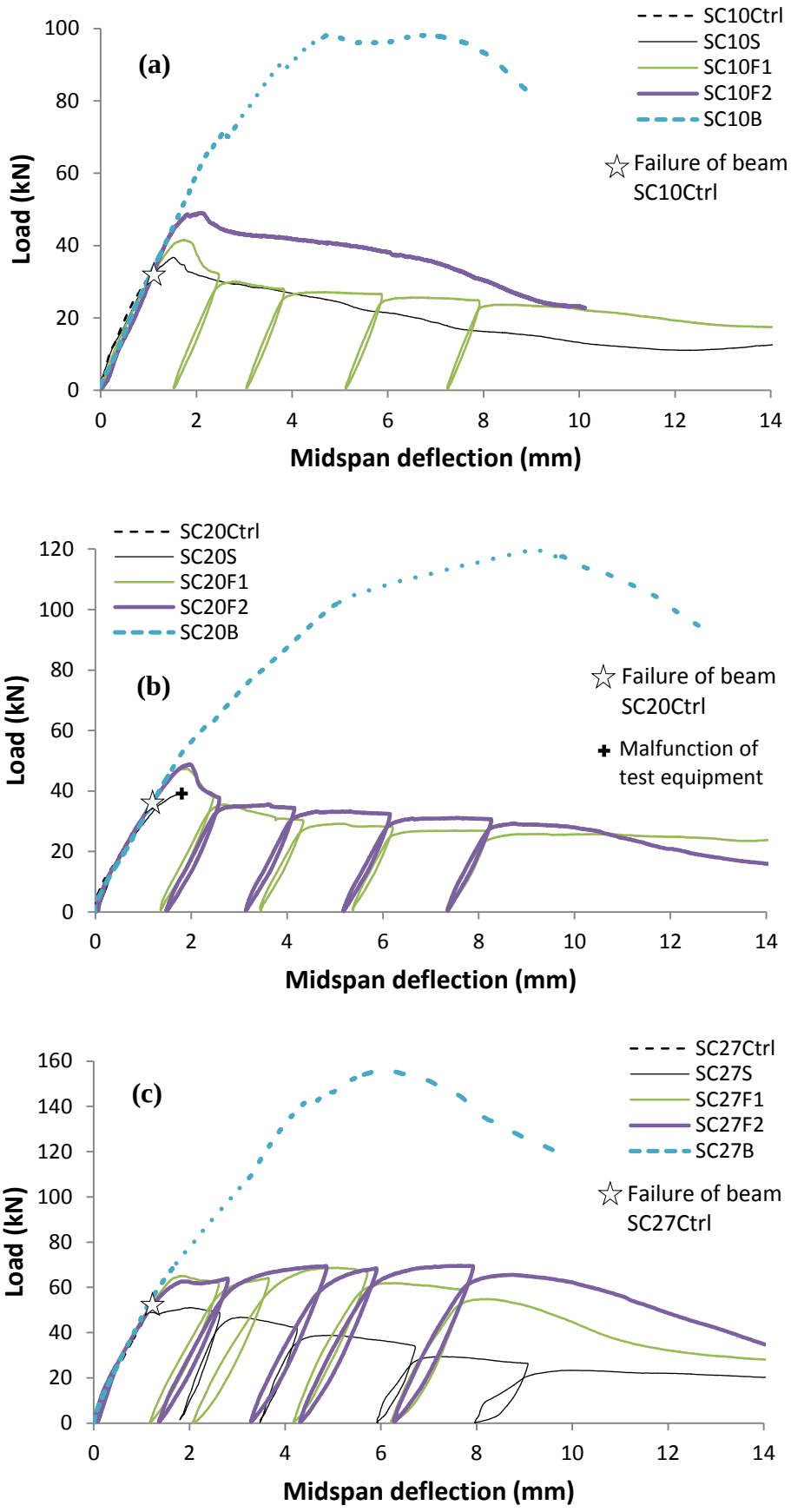

Fig. 4 Load-midspan deflection response of tested beams (a) SC10, (b) SC20, and (c) SC27

In the figures, the brittle failure of the unconfined beams is indicated by a star symbol. The use of internal confinement in the lapped zone led to a ductile response, characterised by a gentle drop of the load capacity after the maximum load. The deflections at splitting of the steel-confined beams increased by up to 62% (beam SC10S) when compared to their unconfined counterparts (see Table 4). However, the steel-confined beams resisted similar or only slightly higher loads than the unconfined beams (by up to 13%). It should be noted that Figure 4b shows the experimental response of beam SC20S only up to splitting failure due to a malfunction of the test equipment.

CFRP confinement was very effective at improving the load-deflection behaviour of the beams by delaying the splitting failure. For all CFRP-confined beams, maximum splitting loads and deflections were consistently higher compared to their unconfined and steel-confined counterparts. As shown in Table 4, splitting loads increased by up to 51% with reference to the unconfined specimens (beam SCF10). Beams confined with 2 CFRP layers sustained higher loads than those confined with 1 layer. Note that Figure 4c shows that, after the splitting of the cover between the bars, the load resisted by the CFRP-confined beams SC27 increased slightly. The slight increase in load capacity was also observed on similar beam tests performed by Harajli (2006). The use of CFRP confinement also increased the deflection at splitting failure by up to 110% (beam SC10F2). After splitting, at 85% of the splitting load, the loads and deflections were up to 39% and 160% higher than those of steel-confined specimens, respectively (except for beams SC10S and SC10F1, which had similar deflections).

Figure 5 shows that CFRP confinement was more effective at increasing the splitting load and deformation capacities as the minimum side/bottom concrete cover decreased ($c_{min(x,y)}$). This suggests that the confining effect of the CFRP sheets is more effective as the cover reduces. A similar trend was reported in experiments on RC columns (Harajli and Dagher 2008).

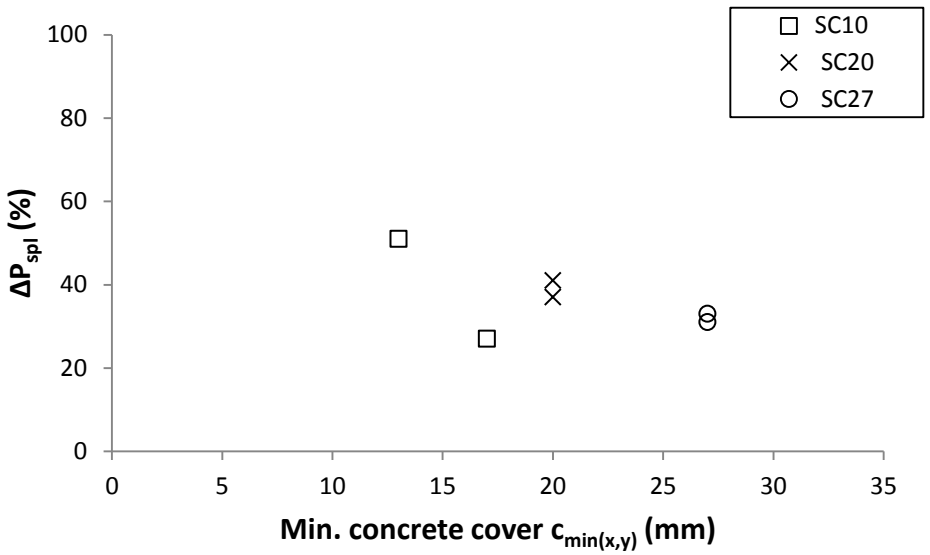

Fig. 5 Effect of minimum concrete cover on load capacity enhancement

3.3 Bond-slip behaviour

The bond stress-bar slip (bond-slip) relationship of the lapped bars provides an insight into the effect of confinement. The average bond stress τ of a bar in tension can be determined assuming that bond is uniformly distributed over the lap length l_b, according to:

$$\tau = \frac{f_s d_b}{4 l_b} \qquad (1)$$

where f_s is the bar stress and d_b is the bar diameter. In the tested beams, f_s was computed using readings from strain gauges fixed on the bars and the corresponding elastic modulus of the bars. Bar slip was obtained from the average readings of the linear potentiometers located at the unloaded ends of the bars, as shown in Figure 2b.

The bond-slip relationships for the tested beams are shown in Figures 6a-c. To compare the results in Figure 6a, bond stresses of beam SC10F1 are normalised by $(22.5/37.6)^{1/4}$. For clarity, only the envelope responses are presented. It is shown that the bond-slip curves are consistent with the corresponding load-deflection responses (see Figure 4a-c). Some minor differences exist between load-deflection and bond-slip curves due to slight variations of effective beam depths and strain gauge readings. The results confirm that the beam failure depends on the bond behaviour of the lapped bars.

Figures 6a-c show that, at the initial loading, the bond-slip relationships of all beams were similar and negligible bar slips occurred. In the CFRP-confined beams, significant concrete cover splitting occurred at bond stresses of approximately 70-90% the bond splitting strength. After splitting and for the same slip value, the bond stress sustained by the CFRP-confined beams was consistently higher due to the delay in splitting crack propagation. In general terms, beams confined with 2 CFRP layers showed a better response than those confined with 1 layer.

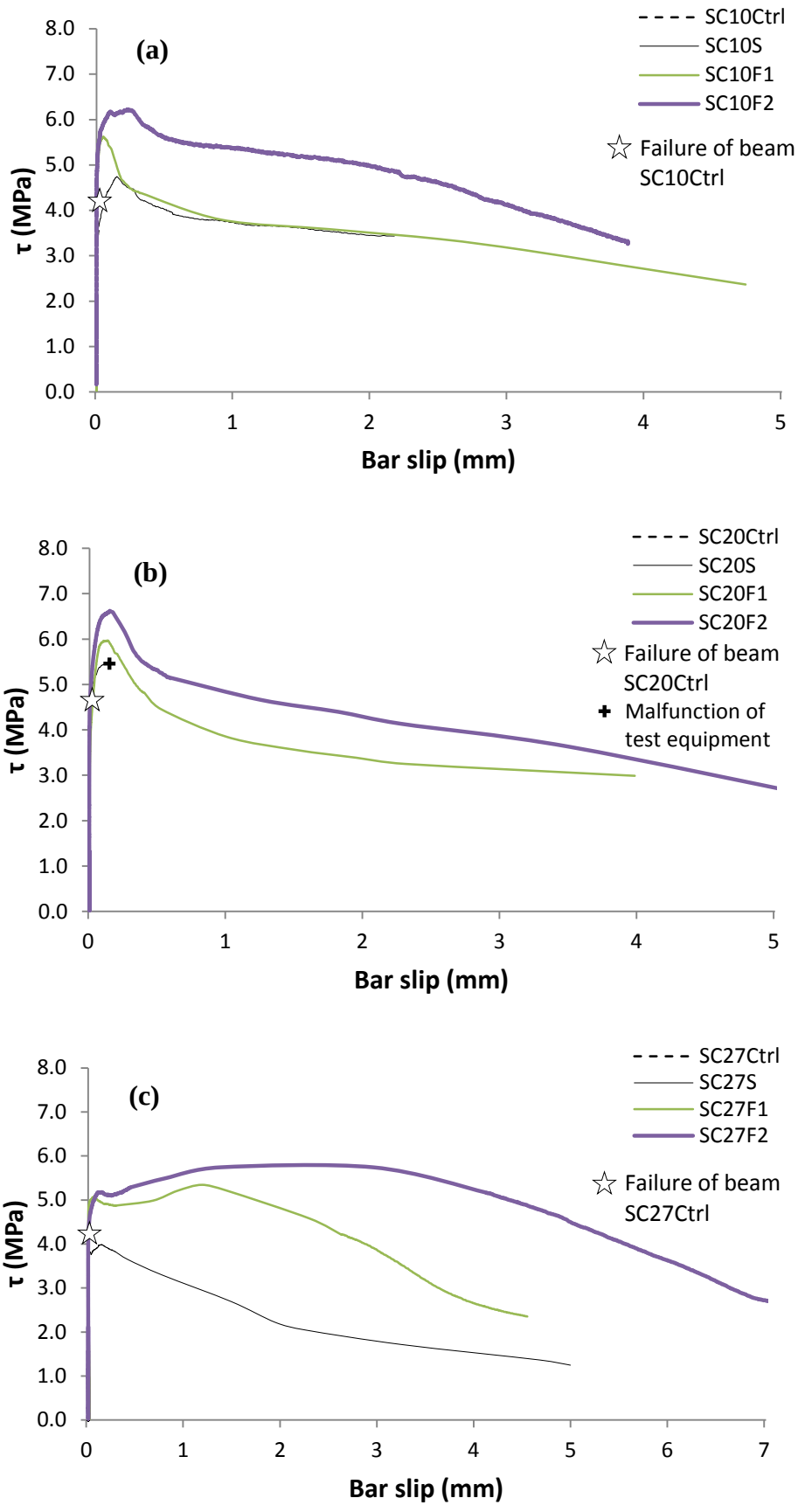

Fig. 6 Bond-slip relationships of tested beams (a) SC10, (b) SC20, and (c) SC27

Table 5 summarises the results of the tested beams at peak load: a) bond strength τ_{spl}, b) bond strength enhancement due to confinement $\Delta\tau_{spl}$, c) normalised bond strength enhancement $\Delta\tau^{*}_{spl}=\Delta\tau_{spl}/\sqrt{f_c}$, d) bar slip s_{spl}, e) bar slip enhancement due to confinement Δs_{spl}, and f) strain in the CFRP confinement $\varepsilon_{f,spl}$. $\Delta\tau_{spl}$ was computed as the difference between the bond strength of the confined beams and that of the corresponding unconfined control beam. To evaluate the effect of confinement at the approximate onset of splitting failure, the CFRP strains at bar slips s=0.01 mm and 0.02 mm are also included in Table 5 ($\varepsilon_{f,s=0.01}$ and $\varepsilon_{f,s=0.02}$, respectively) and Figure 7. The reported CFRP strains are the average readings from the strain gauges shown in Figure 2c. The values of the strain gauges did not differ by much for bottom splitting (as can be seen from Fig. **7**), although they differed for side splitting. Note that the values $\varepsilon_{f,spl}$ reported in Table 5 are only 4-7% of the ultimate strain reported by the CFRP sheet manufacturer (ε_{fu}=1.60%). As shown in Table 5, the premature failure of the unconfined beams is clearly reflected on the very low bar slip values recorded during the tests (0.01 to 0.026 mm only). Although the bond strength of the steel-confined beams was similar or slightly higher than that of the unconfined beams, the use of steel stirrups enhanced the bar slip at failure by up to 590% (beam SC27S). The results also emphasise the effectiveness of CFRP confinement at improving the bond-slip behaviour of the beams. Compared to unconfined specimens, the normalised bond strength was enhanced by up to 33% and 49% for 1 and 2 CFRP confinement layers, respectively. Moreover, the CFRP confinement increased considerably the slip at splitting failure by a minimum of 100% (beam SC10F1) and up to 1200% (beam SC27F2).

Table 5 Bond-slip and CFRP strain results of tested beams

Beam	τ_{spl} (MPa)	$\Delta\tau_{spl}$ (MPa)	$\Delta\tau^*_{spl}$[(b)] ($\sqrt{}$MPa)	$\Delta\tau^*_{spl}$ (%)	s_{spl} (mm)	Δs_{spl} (%)	$\varepsilon_{f,s=0.01}$ (με)	$\varepsilon_{f,s=0.02}$ (με)	$\varepsilon_{f,spl}$ (με)
SC10Ctrl	4.19	-	-	-	0.026	-	-	-	-
SC10S	4.74	0.56	+0.12	+13	0.15[(c)]	NA	-	-	-
SC10F1	5.59[(a)]	1.40	+0.23	+33	0.05	+100	199	363	1170
SC10F2	6.23	2.04	+0.43	+49	0.10	+280	120	193	1030
SC20Ctrl	4.62	-	-	-	0.02	-	-	-	-
SC20S	5.47	0.85	+0.14	+18	0.14	+520	-	-	-
SC20F1	5.97	1.34	+0.22	+29	0.13	+490	60	77	775
SC20F2	6.62	2.00	+0.33	+43	0.15	+570	44	73	570
SC27Ctrl	4.21	-	-	-	0.01	-	-	-	-
SC27S	4.05	-0.16	-0.03	-4	0.07	+590	-	-	-
SC27F1	5.34	1.14	+0.19	+27	0.07	+560	147	211	615
SC27F2	5.75	1.54	+0.25	+37	0.14	+1200	86	119	695

[(a)] Value normalised by $(22.5/37.6)^{1/4}$

[(b)] Bond strength enhancement normalised by $\sqrt{f_c}$

[(c)] Unreliable value due to movement of the measuring equipment

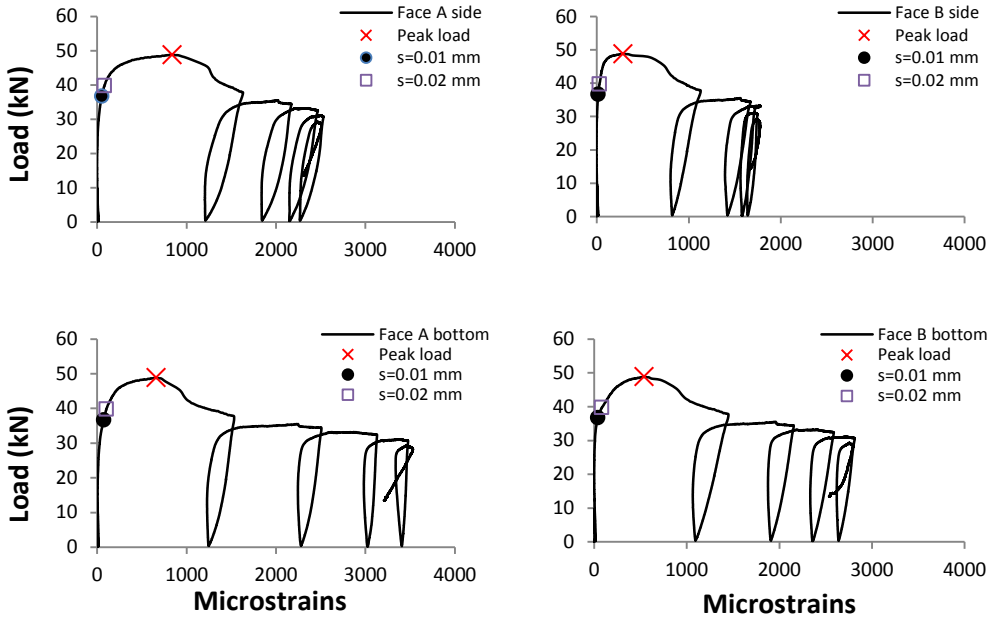

Fig. 7 Typical development of CFRP strains (beam SC20F2)

4. Discussion and comparison of results

4.1 Bond strength of unconfined and steel-confined beams

Table 6 compares the experimental bond strength results of the unconfined and steel-confined beams with predictions by Orangun et al. (1977), Esfahani and Rangan (1998), Zuo and Darwin (2000), Harajli (2006), Lettow and Eligehausen (2006) and EC2 (2004) equations. The (unfactored) predictions by EC2 are computed using the characteristic tensile strength of concrete ($f_{ctk,0.05}$=0.7f_{ctm}). In general, the analytical predictions compare reasonably well with the test results of the unconfined control beams, with Orangun et al., Harajli and EC2 equations giving the best predictions. However, most of the examined models overestimate the contribution of the internal stirrups. This is particularly evident for Zuo and Darwin and Lettow and Eligehausen models, which overestimate the bond results by up to 90% (beam SC27S). It should be mentioned that this may be a characteristic of substandard RC structures, in which internal stirrups may contribute little to bond strength. This is also recognised by current codes (e.g. ACI 318-11 2011), where the internal confinement can be conservatively neglected in bond calculations. Nonetheless, even substandard stirrups can enhance the ductility of laps by providing some bond stress reserve after splitting failure. This is important during earthquakes where structures should be able to

sustain significant deformations. Overall, the results in Table 6 show that the bond splitting strength of substandard splices can be computed with sufficient accuracy using existing bond equations. The good predictions given by equation by EC2 as well as by other researchers (Tepfers 1973, Esfahani and Rangan 1998; *fib* Bulletin 10 2000) confirm that splitting failures are essentially controlled by the tensile strength of concrete. Therefore, the use of the tensile concrete characteristics appears to provide a suitable starting point for the analysis of bond-splitting failures.

4.2 Bond strength enhancement in CFRP-confined beams

To assess the accuracy of existing models at predicting the bond strength enhancement due to CFRP confinement, Table 7 compares the experimental normalised bond strength ($\Delta\tau^*_{spl}$) with analytical predictions ($\Delta\tau^*_{spl,pred}$) by Hamad et al. (2004), Harajli et al. (2004) and Bournas and Triantafillou (2011) bond equations. The table also summarises the predicted effective CFRP strains ($\varepsilon_{f,pred}$) used for the calculation of $\Delta\tau^*_{spl,pred}$ in Hamad et al. and Bournas and Triantafillou equations. The test/prediction ratios (T/P) and corresponding standard deviation (StdDev) for each equation are also reported. Table 7 includes results of normal-strength concrete beams (series NC) tested by Hamad et al. (2004). The short-spliced beams NC were tested under similar conditions as the current beams, but they had different test parameters (e.g. free cover=d_b=20 mm and three lap splices) and less CFRP confinement at midspan consisting of discontinuous or continuous U-shaped strips. It should be noted that Harajli et al. and Hamad et al. equations were calibrated using the test results of beams NC.

Table 6 Summary of test results and analytical predictions according to different bond equations, unconfined and steel-confined beams

Beam	τ_{spl} (MPa)	Orangun et al. (1977) (MPa)	Esfahani and Rangan (1998)[(a)] (MPa)	Zuo and Darwin (2000) (MPa)	Harajli (2006) (MPa)	Lettow and Eligehausen (2006) (MPa)	EC2 (2004) (MPa)
SC10Ctrl	4.19	3.83	4.47	4.78	4.10	4.82	4.14
SC10S	4.74	5.21	-	7.10	5.08	6.83	5.08
SC20Ctrl	4.62	5.59	6.64	5.92	6.50	6.13	4.43
SC20S	5.47	7.25	-	9.08	7.44	8.61	6.11
SC27Ctrl	4.21	4.36	4.83	5.97	4.06	5.00	4.43
SC27S	4.05	5.99	-	7.70	5.24	6.58	4.16

[(a)] Model applicable to unconfined specimens only

Table 7 Test results and analytical predictions of bond strength enhancement, CFRP-confined beams

Beam	$\Delta\tau^*_{spl}$ (√MPa)	Hamad et al. (2004)			Harajli et al. (2004)		Bournas and Triantafillou (2011)[b]			Proposed model		
		$\varepsilon_{fe,pred}$[a] (με)	$\Delta\tau^*_{spl,pred}$ (√MPa)	T/P	$\Delta\tau^*_{spl,pred}$ (√MPa)	T/P	$\varepsilon_{fe,pred}$ (με)	$\Delta\tau^*_{spl,pred}$ (√MPa)	T/P	$\varepsilon_{f,o}$ (με)	$\Delta\tau^*_{spl,pred}$ (√MPa)	T/P
NC1S1	0.08	4000	0.06	1.34	0.03	2.58	-	-	-	74	0.08	1.03
NC1S2	0.09	4000	0.12	0.76	0.06	1.46	-	-	-	77	0.11	0.81
NC1S3	0.18	4000	0.24	0.75	0.12	1.44	3460	0.10	1.80	79	0.16	1.11
NC2S1	0.10	2930	0.09	1.12	0.06	1.58	-	-	-	85	0.12	0.83
NC2S2	0.14	2930	0.18	0.77	0.12	1.09	-	-	-	74	0.16	0.87
NC2S3	0.24	2930	0.25	0.97	0.25	0.97	3460	0.19	1.24	76	0.22	1.08
SC10F1	0.23	4000	0.25	0.91	0.29	0.78	5950	0.40	0.57	86	0.23	0.97
SC10F2	0.43	4000	0.25	1.72	0.40	1.07	5950	0.36	1.19	94	0.37	1.15
SC20F1	0.22	4000	0.25	0.88	0.29	0.75	5950	0.41	0.53	86	0.22	0.98
SC20F2	0.33	4000	0.25	1.31	0.40	0.82	5950	0.47	0.69	86	0.32	1.03
SC27F1	0.19	4000	0.25	0.74	0.22	0.84	5950	0.26	0.72	86	0.19	0.96
SC27F2	0.25	4000	0.25	1.01	0.40	0.63	5950	0.41	0.61	86	0.27	0.92
Mean				1.03		1.17			0.92			0.99
StdDev				0.30		0.54			0.45			0.11

[a] Computed using ACI 440.2R (2008) guidelines for shear strengthening

[b] Using the modified Lettow and Eligehausen (2006) approach. Model applicable to full FRP confinement along the lap only

As expected, Hamad et al. equation predicts the test data used for its calibration with reasonably accuracy, but it underestimates the results of beams SC confined with 2 CFRP layers by up to 72%. This can be attributed to the conservative upper limit of normalised bond strength enhancement adopted in this model ($\Delta\tau^*_{spl}$=0.25). This limit was originally proposed by Orangun et al. (1977) for spliced beams confined with internal steel stirrups and acknowledges that, after a certain point, adding stirrups is no longer effective at enhancing the lap bond strength as bar pullout tends to dominate the failure. The relatively high variability of the test/prediction ratios (StdDev=0.30) reflects the conservativeness of the equation at high confinement levels.

In comparison, Harajli et al. and Bournas and Triantafillou equations predict the experimental results of some beams SC with reasonably accuracy, but they generally underestimate the results of beams NC by up to 158% and 80%, respectively. Moreover, the large scatter of test/prediction ratios (StdDev=0.54 and 0.45, respectively) indicates that these models do not capture accurately the influence of CFRP confinement on bond. The upper limit of normalised bond strength enhancement for EBR suggested by Harajli et al. ($\Delta\tau^*_{spl} \leq 0.40$) appears to be more appropriate than the more conservative limit proposed by Hamad et al. This is consistent with the experimental observations which show that CFRP confinement controls splitting cracks more effectively than internal steel confinement. Based on Harajli et al. observations and on the current test results, it is apparent that the use of additional CFRP layers is not expected to enhance considerably the bond strength by more than $\Delta\tau^*_{spl}$ =0.40. Therefore, it is uneconomical to provide more confinement than that necessary to develop the full bond strength of the lap (unless it is required for other strengthening objectives). This means that the use of suitable bond equations in the design of FRP strengthening of lapped RC members can lead to more economical solutions.

The test results also show that the bond strength of beams confined with 2 CFRP layers was 32-85% higher than that of beams confined with 1 layer only (see also Table 5). Hence, increasing the thickness of CFRP confinement does not result in proportional enhancement of bond strength, as shown in Figure 8. This is in agreement with previous experimental results by Hamad et al. (2004). Despite the

significant bond improvement, CFRP-confined beams sustained 40 to 50% of the load resisted by the corresponding benchmark beams with continuous main bottom bars (see Table 4). This indicates that CFRP confinement can enhance the capacity of substandard splices, but that enhancement could be still insufficient to develop yielding in very short splices.

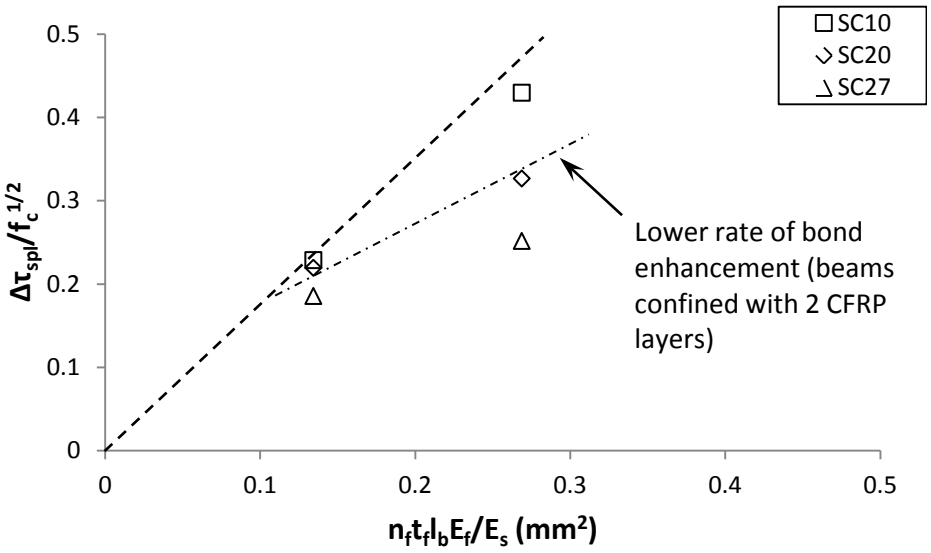

Fig. 8 Normalised bond strength vs amount of CFRP confinement

4.3 Strains developed in CFRP confinement

To compute the bond strength enhancement due to CFRP confinement, the Hamad et al. and Bournas and Triantafillou models require calculating the effective CFRP strain at splitting failure. For the beams tested in this research, the models predict CFRP strains values of 4000 and 5950 με, respectively (see Table 7). However, the current test results show that splitting failures occur at much lower CFRP strains (see Table 5). As strains in the CFRP confinement depend on bar slip and consequent concrete dilatancy, the bond-slip relationship of the bars and the development of CFRP strains during the tests are examined in more detail.

Figures 9a-b show the development of CFRP strain and bar slip as a function of bond stress for beam SC20F2. These are typical results and the following observations apply to the other beams as well. Figure 9a indicates that CFRP strains are very small during the initial loading and up to approximately 50-60% of the bond splitting strength. This was expected as bar slip is practically

negligible at low load levels (see Figure 9b), and therefore the CFRP confinement is not activated. At an approximate bar slip of 0.01 mm, concrete dilatancy around the bar has activated the confinement, thus mobilising strains in the CFRP sheets. CFRP strains increase rapidly as the splitting cracks widen at 70-90% of the bond splitting strength (0.01 mm≤s≤0.1 mm, see Figure 9a). Bond stress remains practically constant before and after splitting failure (marked by × in Figures 9a-b). Following splitting, CFRP strains increase rapidly up to approximately 1000 με, due to additional bar slippage and consequent widening of cracks. Large CFRP strains in excess of 2500-3000 με are recorded only towards the end of the tests when the bars pullout completely from the concrete. Such strains are only 15-19% of the ultimate strain reported by the CFRP sheet manufacturer (ε_{fu}=1.60%). It should be noted that the gauges bonded to the CFRP sheets only provide local strain data. Therefore, the increase in strain values shown in Figures 7 and 9(a) is mainly attributed to widening of splitting cracks along the lapped bars.

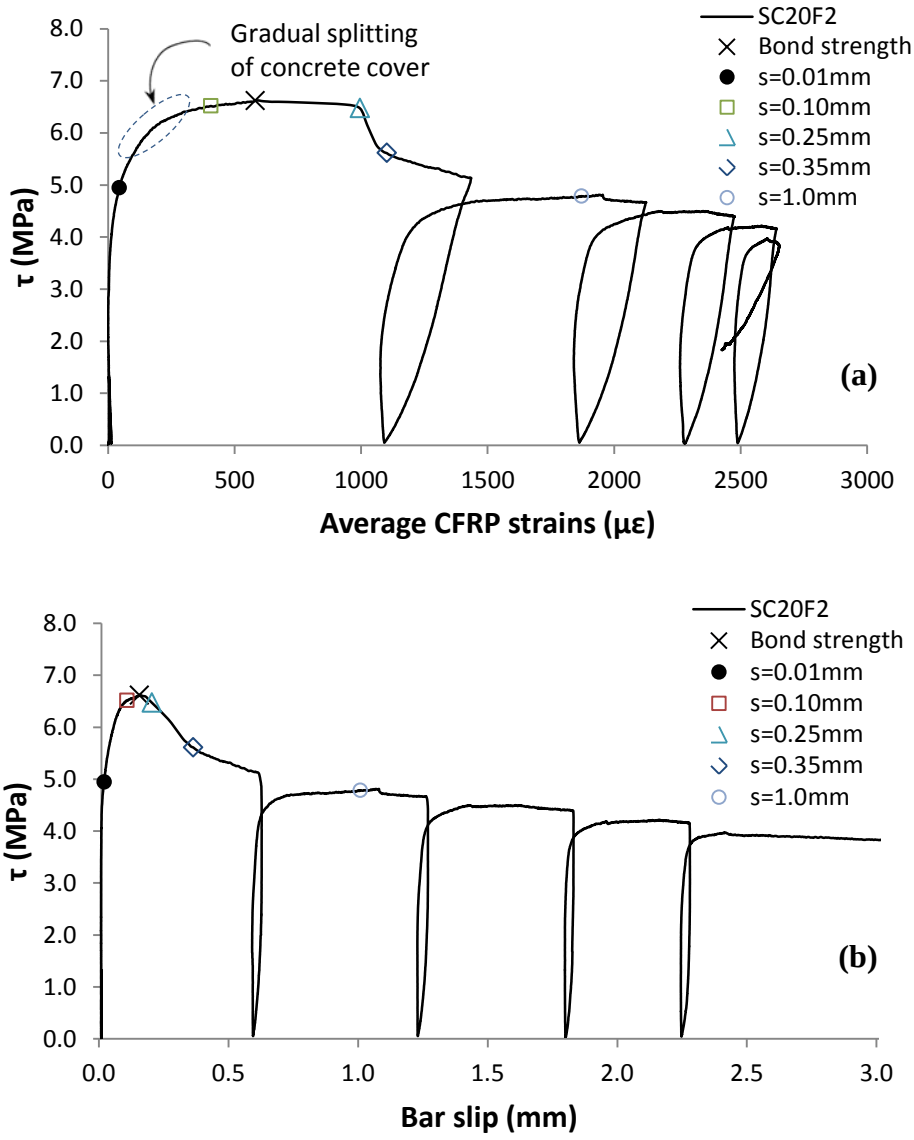

Fig. 9 Typical test results of (a) strains in CFRP confinement, and (b) bond-slip (beam SC20F2)

Based on the above discussion, it is evident that splitting failures occur at small bar slips and low strain values in the CFRP confinement. For the CFRP-confined beams tested in this research, CFRP strains never exceeded 1500 με at peak load. This is less than 10% of the ultimate elongation capacity of the CFRP sheets. Harajli and Dagher (2008) measured similar values of 100-1300 με in tests on lap spliced columns confined with 1 or 2 layers of CFRP. Using a kinematic relationship between bar slip and concrete cover dilation, Tastani and Pantazopoulou (2007; 2008) also computed CFRP strains in the order of 1000-1600 με. The results of these three studies indicate that Hamad et al. and Bournas and Triantafillou models overpredict considerably the strain values of the CFRP confinement. It should be mentioned that more tests are necessary to determine

the appropriate CFRP strains developed at splitting failure for longer splices. The authors will be presenting such results in a separate paper.

5. Model proposal

The large scatter and inconsistencies of existing predictive equations indicate the need for more accurate analytical models for the CFRP strengthening of substandard laps. This is particularly important for the strengthening of structures in developing countries as lower strengthening costs would make rehabilitation of structures more likely. Hence, a new approach for predicting the bond strength enhancement of substandard lapped bars due to CFRP confinement is proposed in the following.

In the proposed approach, the concrete around the lapped bars is regarded as two thick-walled cylinders of thickness $c_{min(x,y)}$ (e.g. Tastani and Pantazopoulou 2007; 2008) as shown in Figure 10a, where side splitting is considered as an example of cover splitting. It is also considered that the initial behaviour of the splice is mainly controlled by the tensile concrete characteristics of the cover. Due to the high variability in concrete strength characteristics in tension, splitting failures of unconfined laps occur when the characteristic tensile stress in the concrete cover (perpendicular to the splitting crack) is exceeded (see Figure 10a). The strengthening of a lap with CFRP confinement is expected in the first instance to reduce the concrete variability in tension and, as a result, splitting in the CFRP-confined lap is expected to be governed by the mean tensile strength of concrete f_{ctm} (see Figure 10b), rather than the characteristic strength.

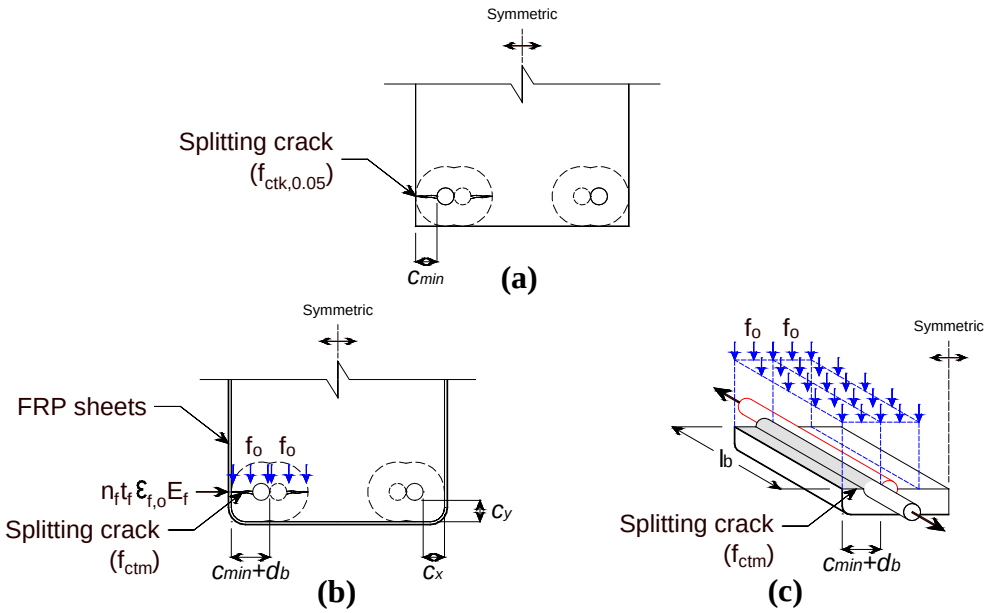

Fig. 10 Bond-splitting failure assumptions in (a) unconfined lap, (b) CFRP-confined lap and (c) confining pressure of CFRP sheets on lapped bar

The additional effect of the CFRP confinement can then be considered through an additional confining stress, f_o, which is assumed to act over a split cross sectional area equal to $(c_{min(x,y)}+d_b)\cdot l_b$ (see Figure 10c). A strain control approach is adopted to compute f_o, which leads to Equation (2). The effective CFRP strain $\varepsilon_{f,o}$ is calculated using the concrete tensile strain at the onset of cover splitting (see Figure 10b), when concrete tensile strains (ε_{ctm}) and CFRP strains are assumed to be equal. Hence, $\varepsilon_{f,o}=\varepsilon_{ctm}=f_{ctm}/E_{cm}$, where all the variables were defined before. With exception of beam SC10F1, Table 7 shows that the predicted values $\varepsilon_{f,o}$ compare reasonably well with the experimental CFRP strains at the approximate onset of splitting (see values $\varepsilon_{f,s=0.01}$ and $\varepsilon_{f,s=0.02}$ in Table 5). f_o is defined by:

$$f_o = \frac{n_f t_f \varepsilon_{f,o} E_f}{n_b (c_{\min(x,y)} + d_b)} \qquad (2)$$

where n_f and t_f are the number of CFRP sheets and thickness of one sheet, respectively; E_f is the elastic modulus of the CFRP; n_b is the total number of pairs of lapped bars in tension (included in Equation (2) to account for the number of splitting cracks), and the rest of the variables are as defined before. For discontinuous CFRP applications (strips), Equation (2) can be multiplied by w_f/s_f, where w_f and s_f are the width and spacing at centres of the CFRP strips, respectively.

It should be mentioned that Equation (2) assumes that the bond strength enhancement provided by the CFRP confinement is related to the elastic strain in the concrete, and cover splitting leads very rapidly to splitting failure. Although the development of a splitting crack along the lapped bars is not instantaneously leading to splitting failure, this assumption is sufficiently accurate to predict the bond strength enhancement provided by the CFRP confinement for the beams tested in this study, where cover splitting occurred at 70-90% of the lap bond strength. Also, note that the CFRP sheets provide passive confinement and therefore their contribution depends on concrete dilation around the lapped bars. Such confining stress is mobilised even at very low slip values (<0.01 mm). This is confirmed by the strain readings from the gauges bonded to the CFRP sheets (Figure 9a). The proposed equation predicts an increase of the contribution of CFRP confinement to bond strength with a reduction of the minimum concrete cover $c_{min(x,y)}$, as also observed in the experiments (Figure 5).

Based on a calibration with the test data of beams NC and SC, the relationship between the bond strength enhancement due to CFRP confinement and the confining pressure can be defined by the following equation:

$$\Delta\tau_{spl}^{*} = \frac{\Delta\tau_{spl}}{\sqrt{f_c}} = 1.15\sqrt{f_o} \le 0.40 \qquad (3)$$

In Equation (3), the maximum bond enhancement is limited to $0.4\sqrt{f_c}$ as shown by the current tests and as proposed by Harajli et al. (2004).

Figure 11 compares the experimental results of beams SC and NC with Equation (3). The concrete tensile strength of beams SC was taken from the test data reported in Table 2, whilst the strength f_{ctm} of beams NC was calculated using EC2. It can be seen that the proposed equation matches well the experimental results. The bond predictions given by Equation (3) are reported in Table 7. Compared to other models, it is evident that the proposed equation predicts the test results more accurately (mean T/P=0.99) and with significantly less scatter (StdDev=0.11). Therefore, the proposed approach can be used for assessment and strengthening of short splices in existing substandard RC constructions of developing countries, where members are typically reinforced with no more than two or three bars on each face.

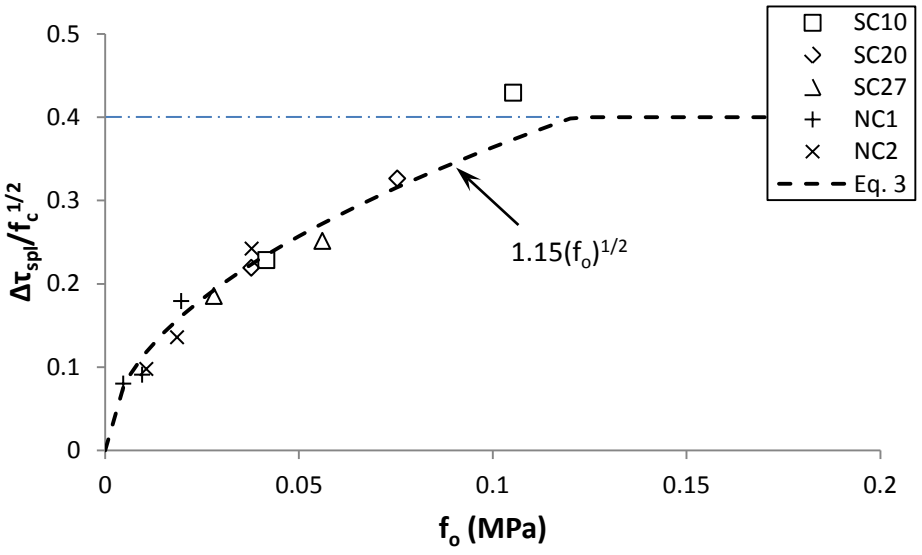

Fig. 11 Proposed equation and fitting of experimental results, CFRP-confined beams

It should be mentioned that Equation (3) needs to be added to the concrete contribution to compute the total bond strength of the lapped bars. As discussed in section 4.1, the concrete contribution can be calculated with sufficient accuracy using existing bond equations available in the literature (e.g. EC2). Due to the limited data used for the calibration and to the short lap length examined, future research should verify the applicability of the proposed model to the CFRP strengthening of RC members with longer laps where yielding can occur. Moreover, as for internal steel stirrups, CFRP confinement is expected to be more effective at engaging bars located at the corners of rectangular cross sections in comparison to intermediate bars. Consequently, further research should also verify the accuracy of the proposed model at predicting the bond strength enhancement in members with more than three splices or with several bars distributed across the section. Also, due to the relatively small number of concrete covers examined in the tested beams, the applicability of the model should be limited to approximately $0.8 \leq c_{min(x,y)}/d_b \leq 2.0$ until future data become available. The use of other FRP materials such as glass, aramid or basalt should be also studied.

6. Conclusions

This paper presented results from substandard splices in RC beams confined with internal steel stirrups or externally bonded CFRP. The beams were subjected to four-point bending and were designed to fail by bond-splitting at midspan, where the main flexural reinforcement was lapped. Based on the results presented in this paper, the following conclusions are drawn:

1) Unconfined control beams with short splices failed in a brittle manner due to splitting of the concrete cover around the splice. For the tested beams, bar slip at splitting ranged from 0.01 to 0.026 mm.

2) Compared to unconfined specimens, steel-confined beams failed by splitting at similar or slightly higher loads (by up to 13%) and bond strengths (by up to 18%). However, bar slips increased by up to 590%. After splitting, steel-confined beams showed a rather ductile behaviour and sustained significant additional deformations, but with a gradual drop in capacity.

3) Existing equations predict the bond strength of substandard unconfined splices with sufficient accuracy, but they tend to overestimate the additional contribution of internal stirrups. Compared to other bond equations, EC2 predicts more accurately the beam test results as splitting is essentially controlled by the tensile concrete strength.

4) The use of externally bonded CFRP confinement delayed the splitting failure of the laps. Compared to unconfined specimens, CFRP confinement also enhanced the bond strength and bar slip by up to 49% and 1200%, respectively. Whilst strengthening applications with 1 or 2 CFRP layers proved very effective at enhancing the splice bond strength, further enhancements are not expected beyond $0.40\sqrt{f_c}$. Therefore, it seems uneconomical to provide more confinement than that necessary to develop the full bond strength of the lap.

5) The test results show that splitting failures of laps in CFRP-confined members occur at small bar slips ($s \leq 0.15$ mm) and relatively low strains in the CFRP confinement (570-1170 με). These values are much lower than the effective CFRP

strains predicted by Hamad et al. (2004) and Bournas and Triantafillou (2011) bond equations (4000-5950 με).

6) Existing equations for predicting the bond strength enhancement due to CFRP confinement show large scatter when compared to experimental results. A new "strain" approach that yields more consistent predictions is proposed. This can be used for assessment and strengthening of short splices in substandard RC constructions.

Acknowledgements The first author acknowledges the financial support provided by Consejo Nacional de Ciencia y Tecnologia (Mexico) and Direccion General de Relaciones Internacionales through its Complementary Scholarship programme. The second author wishes to acknowledge the financial support provided by Damascus University (Syria). The CFRP system was kindly provided by Weber UK.

References

ACI 318-11 (2011) Building Code Requirements for Structural Concrete (ACI 318-11) and Commentary. American Concrete Institute, Farmington Hills, Mich.

ACI 440.2R-08 (2008) Guide for the Design and Construction of Externally Bonded FRP Systems for Strengthening Concrete Structures. American Concrete Institute, Farmington Hills, Mich.

Bournas DA, Triantafillou TC (2011) Bond strength of lap-spliced bars in concrete confined with composite jackets. J Compos Constr 15(2):156-167.

Bousias S, Spathis A-L, Fardis MN (2006) Concrete of FRP jacketing of columns with lap splices for seismic rehabilitation. J Earthq Eng 11(5):653-674.

Breña SF, Schlick BM (2007) Hysteretic behavior of bridge columns with FRP-jacketed lap splices designed for moderate ductility enhancement. J Compos Constr 11(6):565-574.

BSI (2004) BS EN 1992-1-1 Eurocode 2: Design of Concrete Structures Part 1-1: General Rules and Rules for Buildings. British Standards Institution, London, UK.

BSI (2005) BS 4449:2005 Steel for the reinforcement of concrete-Weldable reinforcing steel-Bar, coil and decoiled product-Specification. British Standards Institution, London, UK.

BSI (2005) BS EN 1998-3 Eurocode 8: Design of structures for earthquake resistance Part 3: Assessment and retrofitting of buildings. British Standards Institution, London, UK.

BSI (2009a) BS EN 12390-3:2009 Testing hardened concrete Part 3: Compressive strength of test specimens. British Standards Institution, London, UK.

BSI (2009b) BS EN 12390-5:2009 Testing hardened concrete Part 5: Flexural strength of test specimens. British Standards Institution, London, UK.

BSI (2009c) BS EN 12390-6:2009 Testing hardened concrete Part 6: Tensile splitting strength of test specimens. British Standards Institution, London, UK.

CNR (2004) CNR-DT 200/2004 Guide for the Design and Construction of Externally Bonded FRP Systems for Strengthening Existing Structures. National Research Council, Rome, Italy.
Elgawady M, Endeshaw M, McLean D, Sack R (2010) Retrofitting of rectangular columns with deficient lap splices. J Compos Constr 14(1):22-35.
Elsouri AM, Harajli MH (2011) Seismic repair and strengthening of lap splices in RC columns: carbon fiber-reinforced polymer versus steel confinement. J Compos Constr 15(5):721-731.
Esfahani MR, Rangan BV (1998) Local bond strength of reinforcing bars in normal strength and High-Strength Concrete (HSC). ACI Struct J 95(2):96-106.
fib (2000) Bulletin 10 Bond of reinforcement in concrete. International Federation for Structural Concrete. Laussane, Switzerland.
fib (2010) Bulletin 55 Model Code 2010. Volume 1. First complete draft. International Federation for Structural Concrete. Laussane, Switzerland.
Garcia R, Hajirasouliha I, Pilakoutas K (2010) Seismic behaviour of deficient RC frames strengthened with CFRP composites. Eng Struct 32(10):3075-3085.
Garcia R, Jemaa Y, Helal Y, Pilakoutas K, Guadagnini M (2012) FRP strengthening of seismically deficient full-scale RC beam-column joints. In: Proc. of the 15th World Conf. on Earthq. Eng., Lisbon, Portugal.
Gdoutos EE, Pilakoutas K, Rodopoulos CA (2000) Failure Analysis of Industrial Composite Materials. McGraw-Hill Companies, New York.
Hamad BS, Rteil AA, Salwan BR, Soudki KA (2004) Behavior of bond-critical regions wrapped with fiber-reinforced polymer sheets in Normal and High-Strength Concrete. J Compos Constr 8(3):248-57.
Harajli MH (2006) Effect of confinement using steel, FRC, or FRP on the bond stress-slip response of steel bars under cyclic loading. Mater Struc 39(6):621-634.
Harajli MH, Dagher F (2008) Seismic strengthening of bond-critical regions in rectangular reinforced concrete columns using fiber-reinforced polymer wraps. ACI Struct J 105(1):68-77.
Harajli MH, Hamad BS, Rteil AA (2004) Effect of confinement on bond strength between steel bars and concrete. ACI Struct J 101(5):595-603.
Harajli MH, Khalil Z (2008) Seismic FRP retrofit of bond-critical regions in circular RC columns: Validation of proposed design methods. ACI Struct J 105(6):760-769.
Harajli MH, Rteil AA (2004) Effect of confinement using fiber-reinforced polymer or fiber-reinforced concrete on seismic performance of gravity load-designed columns. ACI Struct J 101(1):47-56.
Harries KA, Ricles JR, Pessiki S, Sause R (2006) Seismic retrofit of lap splices in nonductile square columns using carbon fiber-reinforced jackets. ACI Struct J 103(6):874-884.
Lettow S, Eligehausen R (2006) Formulation of application rules for lap splices in the new Model Code. *fib* Task Group 4.5 "Bond models", Stuttgart, Germany.
Ma R, Xiao Y (1999) Seismic retrofit and repair of circular bridge columns with advanced composite materials. Earthq Spectra 15(4):747-764.
Orangun CO, Jirsa JO, Breen JE (1977) Reevaluation of test data on development length and splices. J Am Concr Inst 74(3):114-122.

Priestley MJN, Seible F (1995) Design of seismic retrofit measures for concrete and masonry structures. Constr Build Mater 9(6):365-377.
Saadatmanesh H, Ehsani MR, Jin L (1996) Seismic strengthening of circular bridge pier models with fiber composites. J Struct Eng-ASCE 91(4):434-447.
Saadatmanesh H, Ehsani MR, Jin L (1997) Seismic retrofitting of rectangular bridge columns with composite straps. Earthq Spectra 13(2):281-304.
Seible F, Priestley MJN, Hegemier GA, Innamorato D (1997) Seismic retrofit of RC columns with continuous carbon fiber jackets. J Compos Constr 1(2):52-62.
Tastani SP, Pantazopoulou SJ (2007) Behavior of corroded bar anchorages. ACI Struct J 104(6):756-766.
Tastani SP, Pantazopoulou SJ (2008) Detailing procedures for seismic rehabilitation of reinforced concrete members with fiber reinforced polymers. Eng Struct 30(2):450-461
Tastani SP, Pantazopoulou SJ (2010) Direct tension pullout bond test: Experimental results. J Struct Eng-ASCE 136(6):731-743.
Tepfers R (1973) A theory of bond applied to overlapped tensile reinforcement splices for deformed bars. Publication No. 73:2. Division of Concrete Structures, Chalmers University of Technology, Goteborg, Sweden.
Youm K-S, Lee Y-H, Choi Y-M, Hwang Y-K., Kwon T-G (2007) Seismic performance of lap-spliced columns with glass FRP. Mag Concr Res 59(3):189-198.
Zuo J, Darwin D (2000) Splice strength of conventional and high relative rib area bars in normal and high-strength concrete. ACI Struct J 97(4):630-641.